International Journal of Modern Physics C
Vol. 23, No. 3 (2012) 1250017 (15 pages)

DOI: 10.1142/S0129183112500179

World Scientific
www.worldscientific.com

MINIMAL TRAFFIC MODEL WITH SAFE DRIVING CONDITIONS

HEINRICH TERBORG* and LUIS A. PÉREZ†

Instituto de Física, Universidad Nacional Autónoma de México
Apartado Postal 20-364, 01000, D.F., México
**hterborg@fisica.unam.mx*
†*lperez@fisica.unam.mx*

Received 3 November 2011
Accepted 18 January 2012
Published 29 March 2012

We have developed a new computational traffic model in which security aspects are fundamental. In this paper we show that this model reproduces many known empirical aspects of vehicular traffic such as the three states of traffic flow and the backward speed of the downstream front of a traffic jam (C), without the aid of adjustable parameters. The model is studied for both open and closed single lane traffic systems. Also, we were able to analytically compute the value of C as 15.37 km/h from a relation that only includes the human reaction time, the mean vehicle length and the effective friction coefficient during the braking process of a vehicle as its main components.

Keywords: Traffic flow; limited deceleration; traffic phase diagrams; traffic safety; coupled-map.

PACS Nos.: 45.70.Vn, 89.40.-a, 05.60.-k, 47.55.-t.

1. Introduction

With the increasing needs for transportation, the financial and environmental impact made by vehicular traffic has also been growing. Thus vehicular traffic has become an important matter of study where traffic engineers and physicists are trying to understand and to improve its management. Achieving this purpose is not just a matter of building bigger highways, but a careful planning of the road's topology and novel technologies are also required.[1] Testing new traffic technologies in real traffic is not always feasible and could be very expensive. With the aid of computer simulations we may assess new technology or, at least, give some insight to its performance. This computational approach requires a computer model capable of recreating real traffic as good as possible within the needed regime. From a physicist point of view a good traffic model should not only be a mere parameter tuning problem, it

† Corresponding author.

must also be the result of incorporating ground aspects of traffic (in the same sense of *first principles* in atomic simulations). By adopting this point of view we should achieve two goals: The first one is to develop a good (realistic) traffic model, and the second, to develop novel technology perfectly suited to a particular system. Cellular automata (CA) models have been recently used in describing traffic flow, since they are able to describe relevant characteristics of the dynamics while keeping computational efficiency and allow to fine control microscopic aspects of the traffic flow.[2] In these models time and state variables are discrete, and there are rules for braking and accelerating that control the movement of the vehicles, but the idea of limited deceleration has seldom been considered in traffic models,[3] and most of the CA ones have imposed arbitrarily large deceleration rates, which can be far beyond the practical braking capability and the realistic driving behavior.[4] A safe distance (Δx) between cars can be written for the steady state as,[3]

$$\Delta x(v) = d_0 + \frac{\alpha_m v^2}{2\mu g} + vT_{\text{reac}}, \tag{1}$$

where v is the vehicle velocity, d_0 is the distance between vehicles in a traffic jam, μ is the effective friction coefficient during the braking process of a vehicle, g is the Earth's gravity constant, T_{reac} is the driver's reaction time and α_m is a constant lower than 1. This constant takes into account any other effects which could affect the safe distance such as the possibility to see through the windshields of other vehicles.[3] This relation for the intervehicle distance takes into account both the limited deceleration of vehicles as well as the driver's reaction time. This safe distance may be considered over-conservative since it supposes that the vehicle is heading for a complete stop, however it is consistent with some empirical facts and shows a good agreement between theory and experimental data without any free parameter (this means $\alpha_m = 1$).[3] With the aid of Eq. (1) it is possible to analytically reproduce to a good extent some aspects of experimental data like the velocity vs headway plot, and other fundamental diagrams.[3]

Taking into account the driver's stochastic behavior,[2,5–7] we present a new model that incorporates safe driving conditions (in a microscopic sense), as well as a stochastic braking parameter p. Since the latter hinders the attainment of any analytical result, we coded these conditions into a cellular automaton model with discrete time that maintains computational efficiency. In the next section we will describe the basic aspects of our model.

The main contribution of this work is the development of a model that takes into account physical acceleration and deceleration limits, in such a way that it is still capable of reproducing basic aspects of real traffic without adjusting any free parameter.

2. The Model

The model is defined over a single highway lane of length L, where the vehicles move from left to right. Each vehicle has a length l_i, and its speed v_i can take any value

between 0 and $v_{\max_i}$. Each car has acceleration a_i and deceleration b_i rates. The position of the ith vehicle is given by x_i and g_i is the ith car's bumper to bumper distance with its leading car. We also define a minimum safe distance $D^i_{\min}(v_i)$ (which could also be a function of any other parameter of the car). The safe distance means that if the ith car is driving with a headway g_i less than $D^i_{\min}(v_i)$, and the leading car suddenly brakes, then the first car may not be able to brake enough to avoid a collision.

As we are only interested in the traffic flow without collisions, we use the following update rules:

(i) If $g_i \leq D_{\min}(v_i)$ then brake safely $v_i = v_{\text{safe}}(g_i)$.
(ii) If $g_i > D_{\min}(v_i)$ then accelerate $v_i \to \min(v_i + a_i \cdot \Delta t, v_{\max})$.
(iii) $v_i \to \max(v_i - b_i \cdot \Delta t, 0)$ with probability p.
(iv) $x_i \to x_i + v_i \cdot \Delta t$.

where Δt is the time-step, and $v_{\text{safe}}(g_i)$ is a function such that $D_{\min}(v_{\text{safe}}(g_i)) = g_i$.

Without any explicit definition for $D_{\min}(v)$ these rules are very general. In this paper we use relation (1) as $D_{\min}(v)$, as this makes the minimum distance a function of the car's own velocity as stated in Eq. (1), and our model inherits the properties of the traffic flow already known from this equation. In this sense, it is important to note that when using Eq. (1) as the safe distance then the limited deceleration capabilities of a vehicle are automatically transferred to the function $v_{\text{safe}}(g_i)$. Moreover, in this paper we use parallel update and, unless stated otherwise, we only consider one type of vehicles, i.e. they all have the same maximum velocity $v_{\max}$, the same size l, and the same acceleration (a) and deceleration (b) constants.

In the next sections, the parameters that characterize a vehicle are taken as mean values for the sake of simplicity and they are summarized in Table 1.

It is interesting to note that the value of d_0 can be obtained from the supposition that a driver always wants to have, at least, the rear bumper of his leading car in sight, and using mean values for the height of the head of a person sitting in a car, the mean distance from the steering wheel to the front bumper and the mean height of a bumper we achieve the same experimental result.

This model naturally limits the deceleration of cars, avoiding unrealistic high values under normal conditions. On the other hand, since this model also avoids

Table 1. Mean values of vehicle parameters.

Vehicle parameter	Symbol	Value
car acceleration[8]	a	$3.02\,\text{m/s}^2$
car deceleration[8]	b	$6\,\text{m/s}^2$
driver's reaction time[3,8]	T_{reac}	$0.8\,\text{s}$
friction coefficient[3,8]	μ	0.8
maximum car velocity	$v_{\max}$	$33\,\text{m/s}$
minimum distance[3]	d_0	$(1.39 \pm 0.44)\,\text{m}$

collisions, setting an initial condition that will surely lead to a collision is the only way to override the limited deceleration.

In this model the values of the distances are continuous within the limit of the computational numerical precision and only time is discretized. The time step is taken as 1 s since this is the order of the reaction time. Generally speaking, this model belongs to the class models which are continuous in space and discrete in time, such as that studied by Krauss *et al.*[9,10] Moreover, both models take into account the limited deceleration capabilities of vehicles but a direct comparison is not possible since Eq. (1) does not explicitly incorporate the velocity of the leading car as in Refs. 9 and 10, but the anticipated behavior is enclosed in the α parameter leading to a simpler set of equations for safe driving.

3. Results

In this section we present the simulation results for this model in both open and closed systems. All simulations are carried out on a road of length $L = 10\,\text{km}$. Each simulation is carried out for $T = 10^6$ time steps after letting the system evolve for a time of $T_0 = 10^6$ time steps.

3.1. *Closed systems*

In the case of a closed system, the car number N remains constant during each simulation, so the mean vehicle density is $\rho = N/L$. Initially, the vehicles are inserted one by one after letting the previously inserted vehicle to drive away, we choose to do so to avoid unrealistic initial configurations. However, we also carried out simulations starting with all the vehicles randomly distributed around the loop and with velocities taking any random value between 0 and $v_{\max}$ and no significant difference was found in comparison with the insertion method described above.

To compare the calculated data from our computer model with the analytical results obtained from Eq. (1) we show the velocity vs headway diagram in Fig. 1. We can see that the simulation matches the analytical result until the maximum allowed speed is reached and the velocity becomes constant.

In Figs. 2 and 3, the fundamental diagram for the proposed model, with different braking probabilities, and different values of α are respectively shown. It is clear from Fig. 2 that the higher the braking probability p is, the smaller the maximum flux (J) will be, and also, the free traffic phase will end at a lower density. It is worth mentioning that very small values of p only soften out the fundamental diagram, leaving it almost unaltered in comparison with that corresponding to $p = 0$. Also notice the appearance of a "shoulder" in the fundamental diagram for $p = 0$ and $\alpha = 1$. This drop in the flux is not a finite-size effect, indeed the jump at this point sharpens when the system size increases, as expected for a phase transition. By looking at the spatiotemporal diagrams, it can be observed that this "shoulder" marks the point where a stable group of cars with zero velocity first appear in the

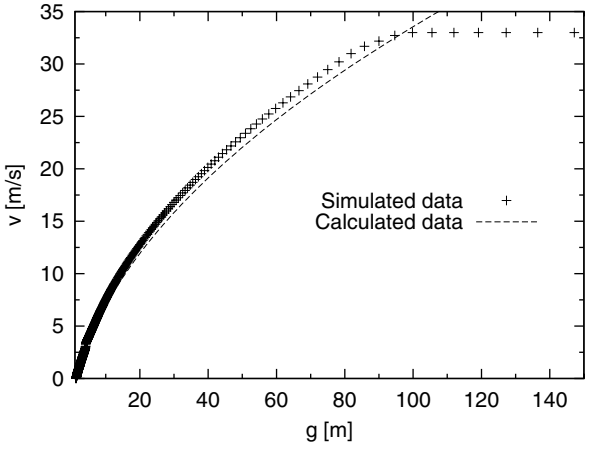

Fig. 1. Velocity vs headway for the model obtained without adjustable parameters (crosses) and its comparison with the analytical curve (dashed line) calculated from Eq. (1) assuming a uniform car distribution.

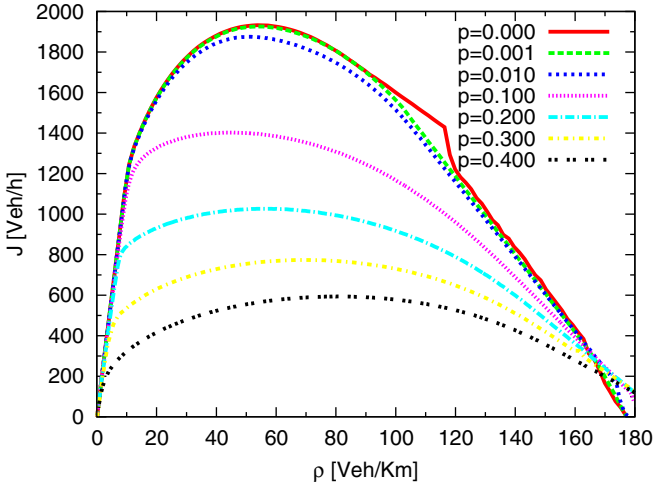

Fig. 2. (Color online) Fundamental diagram of the model with $\alpha = 1$ and different values of p.

steady state. On the other hand, if we perturb the system by adding a non-zero noise then a well defined zero velocity group of cars is not formed and instead we observe the gradual growth of a non-uniform-low-velocity group of cars when density increases.

From Eq. (1) it is clear that α regulates the degree of driver's knowledge and control of the physical braking limitation of the vehicle, thus for small α's the driver is ignoring these limitations and its chosen velocity for a specific headway will not allow him to come to a complete stop in that headway distance. On the other hand, for higher values of α (close to 1), the driver chooses its own velocity as if he has to

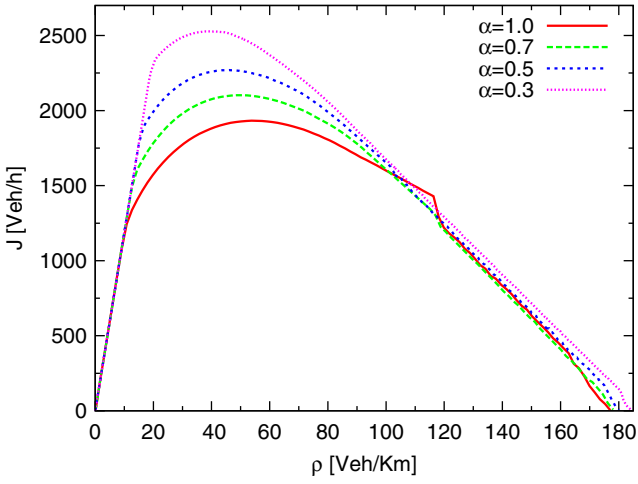

Fig. 3. (Color online) Fundamental diagram of the model with $p = 0$ and different values of α.

make a complete stop in a distance equal to its headway. Notice in Fig. 3 that a smaller value of α accounts for a greater flux as it is expected because this allows the vehicles to travel with the same speed much closer to one another. Indeed, according to Montemayor *et al.*,[3] $\alpha = 0.7$ shows the best correspondence with the experimental data.

In the fundamental diagram (Fig. 2) we can also observe a jump of the flux at about 120 veh/km, this jump is smoothed when α diminishes (Fig. 3), but it almost completely disappears with a non-zero p.

In Fig. 4 we show the data obtained from a virtual detector for the local flux and occupation in the simulations. Observe the bidimensional data dispersion that accounts for the synchronized traffic states, it is important to note that this detector underestimates the density for congested traffic as it only measures those cars that pass through it. In general, from the fundamental diagrams one can observe the existence of free and congested traffic, and the general behavior that is in correspondence with experimental data.[11] However, these diagrams are not sufficient to accurately identify the different types of traffic states and then spatiotemporal diagrams can also be used.[4] As an example, in Fig. 5 we show a spatiotemporal diagram in the congested traffic regime for a closed system with $\rho = 170$ veh/km, $\alpha = 1$ and $p = 0$.

Furthermore, a statistical observable which allows to identify synchronized traffic is the crosscorrelation between the vehicle density ρ and the flow J which is given by[12]

$$CC_{\rho,J}(\tau) = \frac{1}{\sqrt{\sigma_J \sigma_\rho}} (\langle \rho(t) J(t+\tau) \rangle - \langle \rho(t) \rangle \langle J(t+\tau) \rangle), \tag{2}$$

where σ_x denotes the variance of x, and $\langle\,\rangle$ denotes the time average. In synchronized traffic $CC_{\rho,J}(\tau)$ almost vanishes which means that these variables are almost

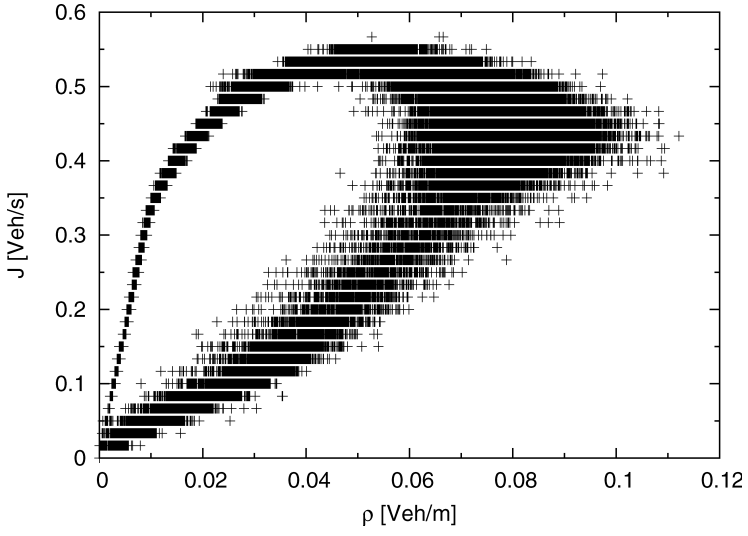

Fig. 4. Local flux versus local density measured with a virtual detector, using one minute averages for a closed system with $p = 0$ and $\alpha = 1$.

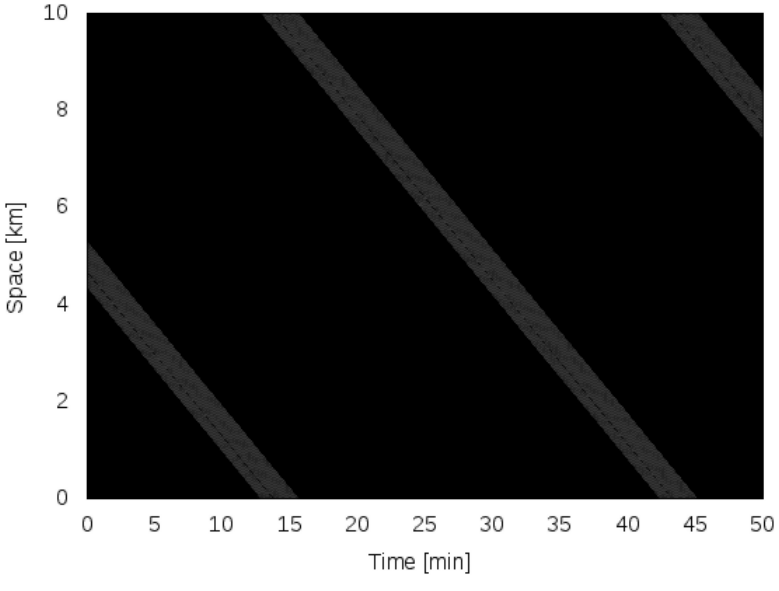

Fig. 5. Spatiotemporal diagram in the congested traffic regime for a closed system with $\rho = 170$ veh/km, $\alpha = 1$ and $p = 0$.

independent from each other. In Fig. 6, we show the crosscorrelation as a function of time for $\rho = 33$ veh/km, with $p = 0$ (solid line with crosses). Note that the oscillations of the crosscorrelation get smaller with time, but they do not vanish completely. This can be explained because when $p = 0$ the system is deterministic, and due to the

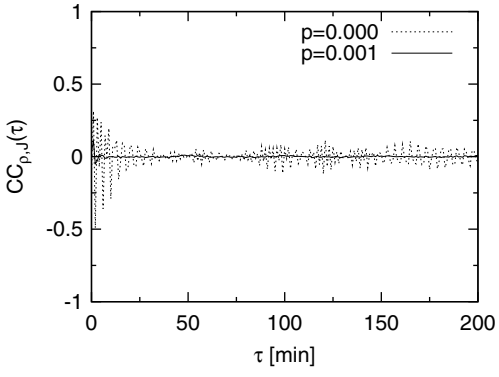

Fig. 6. Crosscorrelation for a closed system with $\rho = 33$ veh/km with $\alpha = 1$, $p = 0$ (gray dashed line) and $p = 0.001$ (black solid line).

periodic boundary conditions we expect to see the same traffic pattern repeating periodically in time when the system has reached its stationary state. However, for the case of $p = 0.001$ (dashed line) the crosscorrelation dies out as expected for synchronized traffic. In general to verify this property of the synchronized traffic within this model, it is sufficient to consider a vanishingly small but non-zero noise parameter. On the other hand, in the Krauss model the synchronized traffic is only achieved by the introduction of an effective maximum acceleration which depends on a new free parameter.[10]

For a closed system with $p = 0$ and $\alpha = 1$, Fig. 7 shows the general trend of the (a) flux (J), (b) velocity standard deviation (σ_v) and (c) $P_v^{\max}$, which is given by

$$P_v^{\max} \equiv \langle (\text{maximum number of cars forming a } v\text{-platoon}) \times v/v_{\max} \rangle. \quad (3)$$

This quantity is the mean value of the maximum number of cars ever seen forming a v-platoon in the simulation times the corresponding velocity (v) and normalized by the maximum velocity ($v_{\max}$). Here, a v-platoon stands for a group of consecutive cars traveling with the same speed (v) within a range of ± 0.5 m/s, regardless of the distance between them. Those 0-platoons which are not actually moving have a zero value of $P_v^{\max}$. As can be seen from Fig. 7(c), the behavior of this quantity shows a high sensitivity to changes in the steady state and then it can be very helpful for determining the nature of traffic states. A large σ_v means that, on average, a vehicle experiences frequent speed changes. In turn, the high speed variance could also increase the probability of traffic accidents. Moreover, a smaller σ_v indicates that the system is less disordered (in the velocity sense). In this way, the analysis of σ_v could allow to draw conclusions about safety and order in the system.[13] Here we can also define an efficiency (η) as $\eta \equiv J/\sigma_v$, which is a good indicator of an ordered high flux under safe conditions. A plot of η as a function of ρ for a closed system with $p = 0$ and $\alpha = 1$ is shown in Fig. 8, where a maximum at a density of $\rho = 8$ veh/km can be observed, together with an almost linear decay for densities greater than 120 veh/km.

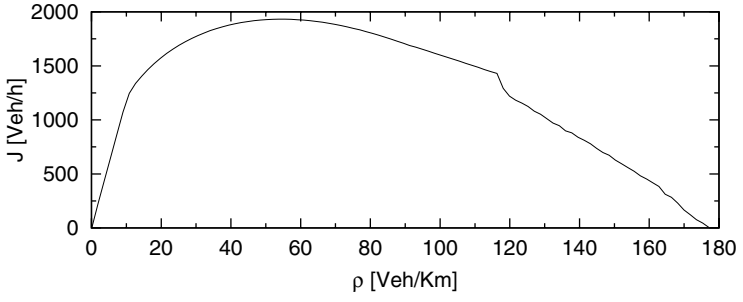

(a)

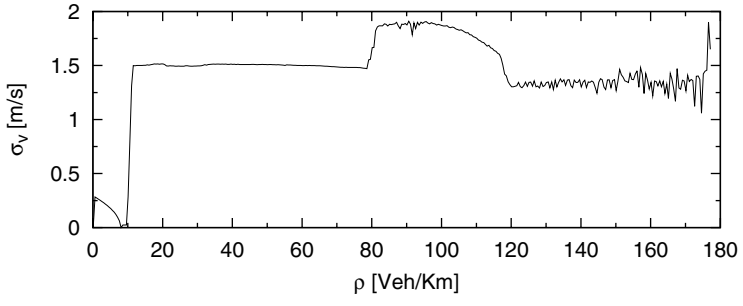

(b)

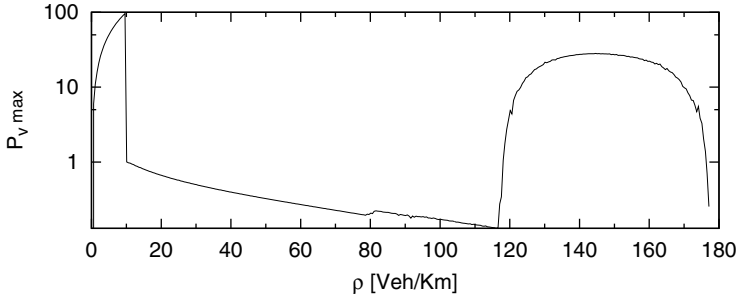

(c)

Fig. 7. (a) Flux (J), (b) velocity standard deviation (σ_v), and (c) $P_v^{\max}$ as a function of the vehicle density (ρ) for a closed system with $p = 0$ and $\alpha = 1$.

In the region between these two values, the efficiency shows an interesting non-monotonic behavior which may be considered in future work.

Another interesting aspect of vehicular traffic is the backward speed of the downstream front of a traffic jam C, which seems to be roughly comparable with a natural constant.[6] In many countries, it has a typical value of $(C = 15 \pm 5)$ km/h, depending on the accepted safe time clearance and average vehicle length.[6] Therefore fully developed traffic jams can move in parallel over long time periods and road

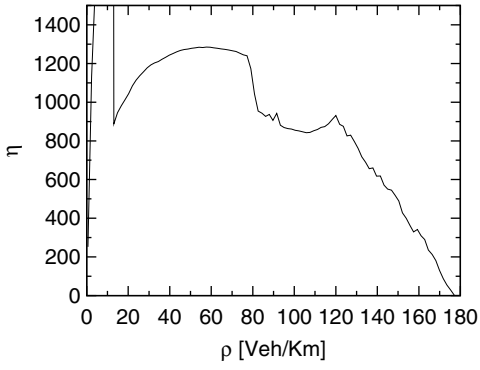

Fig. 8. Efficiency (η) as a function of the vehicle density (ρ) for a closed system with $p = 0$ and $\alpha = 1$.

sections. Their propagation speed is not even influenced by ramps, intersections, or synchronized flow upstream of bottlenecks.[6]

From our simulations we found that this constant C is not altered, at least within the numerical precision, by the car acceleration rate, and that it is very weakly influenced by p. However, we also found a strong dependency with the car sizes (l) and their minimum safe distances (d_0). We measured values for C between 15.3 km/h, and 20.4 km/h for different combinations of car sizes and safe distances. These values are comparable to the reported value of 15 ± 5 km/h.[6]

This constant can be estimated by $(l + d_0)/T_{\text{reac}}$ (which gives ~ 25 km/h) supposing that the first car leaves the jam after a time T_{reac} which leads to a backward motion of the jam front of $l + d_0$. However, this would not take into account the necessary headway for a car to accelerate out of the jam, i.e. a car in the jam has to wait for its leading car to gain enough velocity (and therefore enough distance) before it can also separate from the jam. Since we are in a continuous space/velocity scenario, it would be arbitrary to state whether a car moving away from the jam with infinitesimal velocity and infinitesimal headway from the jam belongs or not to it. Another approach for estimating this constant is by considering the case of a system with periodic boundary conditions where a jam coexists with a uniform car distribution traveling at a speed v_c ruled by Eq. (1). If we think of jam as a region where cars have zero speed and considering that the jam is going to travel backwards with its shape unchanged, we would require that, due to the boundary conditions, the velocity of growth of the jam (how fast cars become part of it) and the velocity of shortening of the jam (how fast they leave the jam) should be the same. Therefore we can couple the equations that describe the uniform states for this system as follows.

From Eq. (1), the time that a car needs to decelerate from a velocity v_c to a velocity $v_0 < v_c$ is given by

$$\tau_{v_c}(v_0) = T_{\text{reac}} + \frac{v_c - v_0}{\mu g}, \tag{4}$$

and the changes in the size of the 0-platoon are given by its growth velocity in the upstream direction, v_{up}, given by

$$v_{\text{up}}\tau_{v_c}(v_0 = 0) = l + d_0, \tag{5}$$

then, the stability condition states that

$$v_{\text{up}} = v_c. \tag{6}$$

Using (6) we obtain

$$\frac{v_c^2}{\mu g} + v_c T_{\text{reac}} = l + d_0, \tag{7}$$

which has only one physical solution given by

$$v^* = \frac{-T_{\text{reac}} + \sqrt{T_{\text{reac}}^2 + 4\frac{l+d_0}{\mu g}}}{\frac{2}{\mu g}}. \tag{8}$$

Substituting the values $T_{\text{reac}} = 0.8\,\text{s}$, $l = 4.35\,\text{m}$, $d_0 = 1.39\,\text{m}$ and $\mu = 0.8$ we obtain

$$v^* \approx 4.27\frac{\text{m}}{\text{s}} = 15.37\frac{\text{km}}{\text{h}}. \tag{9}$$

This last result is again in concordance with the reported value.[6]

3.2. *Open systems*

Until now we have analyzed the behavior of a system in a closed loop where the number of cars remains constant over time. But most of the systems in real world are open, i.e. the number of cars in the system is not constant over time. In order to study this case, simulations were performed where cars were inserted at the beginning of the highway with probability α' and they were removed from the end of the highway with probability β'. The results obtained from these simulations are shown in Fig. 9. In Fig. 9(a) we show the density phase diagram for the open system, where one can observe the existence of a high density region. The corresponding flux diagram is plotted in Fig. 9(b). Notice that inside the high density region, the flux is almost independent of α', whereas outside this region the flux is almost independent of β'. Furthermore, Fig. 9(c) shows the diagram for $P_v^{\max}$, where one can observe the existence of a maximum platooning region, and also that almost no platooning (in the sense defined by Eq. (3)) occurs for the high density and the high flux regions. Finally, a diagram of σ_v is shown in Fig. 9(d). Notice that the high flux and the high density regions share almost the same values of σ_v. Also remarkable is the transition line between the high density and the low density regions, which has a very high value of σ_v. Moreover, in the region of high density the measured parameters depend mostly on β' and they are independent of α' (at least within numerical precision). On the other hand, in the rest of the diagram the main dependence is on α'.

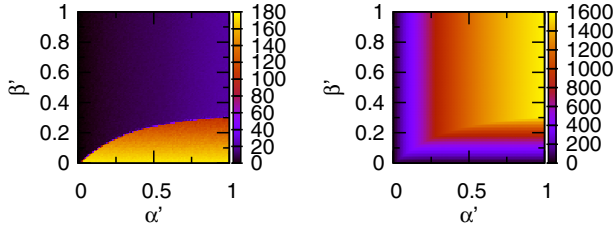

(a) ρ [Veh/km] (b) J [Veh/h]

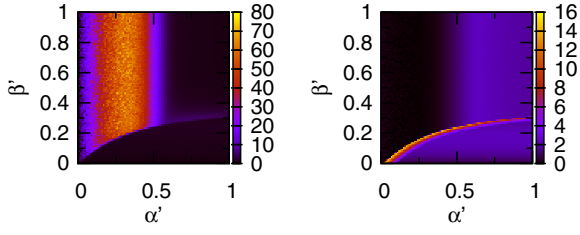

(c) $P_v^{\max}$ (d) σ_v

Fig. 9. (Color online) (a) Density (ρ), (b) flux (J), (c) $P_v^{\max}$, and (d) velocity standard deviation σ_v phase diagrams for an open system of length $L = 10$ km, $p = 0$ and $\alpha = 1$.

In the case of the flux diagram, Fig. 9(b), if we denote the transition line between the high density and the low density regions as $S_{II}(\alpha')$, then for a point $(\alpha'_c, \beta'_c = S_{II}(\alpha'_c))$ that lies on this curve, all the points $(\alpha'_c, \beta' \geq \alpha'_c)$ and $(\alpha' \geq \alpha'_c, \beta'_c)$ share the same flux (within the numerical precision).

In Fig. 10, we have separated the open system phase diagram into regions which we will describe briefly. Region (I) is a very low density one characterized by low input rates $\alpha' \lesssim 0.13$, in this region the cars normally drive at their maximum speed (free traffic), it has a small σ_v, but the headway variance σ_g has its maximum value. Region (II) is a high density one, characterized by low output rates $\beta' \lesssim 0.29$, very small flux and where σ_g has its minimum and σ_v is higher than region (I). In this

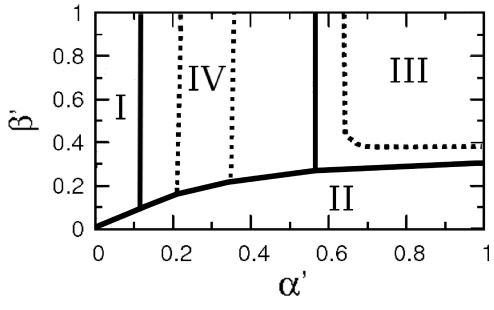

Fig. 10. Phase diagram for an open system with $p = 0$ and $\alpha = 1$. The solid lines separate the different regimes: (I) low density regime, (II) high density regime, (III) maximum flux regime, and (IV) high $P_v^{\max}$ regime. The dashed lines enclose local maxima for $P_v^{\max}$ or J (see text).

region there is very little platooning and practically no platooning at all below $\beta' = 0.05$. Here all measurements are almost independent of α', i.e. their main behavior is only dictated by β'. The densities over the line that separates region (II) from the rest, vary from $\rho \sim 30\,\text{veh/km}$ to $\rho \sim 110\,\text{veh/km}$ (values that are not found elsewhere). For many points over this line we found a vanishing crosscorrelation (see Eq. (2)), suggesting that synchronized traffic states lie all over this line.

Region (III) corresponds to the maximum flux, here the flux grows when α' increases. The zone enclosed by the dashed line in this region ($\alpha' \gtrsim 0.61$ and $\beta' \gtrsim 0.29$) has the overall lowest platooning values together with region (II).

Region (IV) corresponds to those states with the greatest efficiency as defined before. In this region we still have free traffic near the vicinity of region (I) as the flux grows almost linearly with α' (and so with the density) and independently of β'. Also in this vicinity we have the minimum value of σ_v and the overall greatest efficiency for $0.1 \lesssim \alpha' \lesssim 0.2$. In this region, the headway variance σ_g vanishes, σ_v increases with α', and the cars tend to travel in platoons [as defined by Eq. (3)]. The dashed lines in region (IV) (see Fig. 10) enclose the area were the largest and fastest v-platoons are measured. Platooning is found to depend mostly on the injection rate, and it has an overall maximum at $\alpha' \approx 0.33$.

As we approach region (III) from region (IV) the flux slows down its growth with increasing α', and platooning has decreased in comparison with those values found in region (IV) and starts showing a slight dependence on β'. Also, the efficiency abruptly decreases in comparison with the values found in (IV).

We also point out that by increasing the size of the system, the frontier of these regions is sharpened, suggesting that these regions are indeed different phases of the system. It is worth mentioning that similar phase diagrams for ρ and J as a function of the boundary (upstream and downstream) densities can be obtained by applying the extremal principle of Popkov and Schütz[14] to the fundamental diagram of the open system. However, the translation of these diagrams to the $\alpha' - \beta'$ space, as well as the obtention of the phase diagram for $P_v^{\max}$ is not straightforward.

This analysis for an open system as stated here with insertion and extraction probabilities (α', β'), could be used to set dynamic velocity limits along a road in order to maximize the road efficiency during rush hours. Moreover, in comparison with the knowledge obtained from the fundamental diagram, this analysis gives much more information for the path that a system will follow along the region diagrams (Fig. 10) when their in and out flows change. Furthermore, we could even be able to drive the system from an initial state to any other desired state following a path of less velocity variance, thus minimizing the emission of contaminants and the chance of accidents while controlling traffic.

4. Conclusions

We have presented a computational traffic model that includes physical safe driving constraints such as limited acceleration and deceleration, together with the driver's

desire to travel as fast as possible. This model is able to reproduce some known aspects of traffic such as the three states of traffic flow as well as the backward speed of the downstream front of a traffic jam, without having the need to adjust any free parameter. One of the main features is the simplicity of its rules, which attain for a low computational cost, allowing to do calculations faster than real traffic development. Thus, this model is capable of making predictions of the traffic state in the future, given a present traffic state.

This model can be easily extended to include different types of cars, and it could be benefited from parameter adjustment in order to do quantitative predictions. It also provides a base to study the integration of different driving strategies in which safety is a priority, that could lead to a more efficient road usage.

From the results obtained with this model and the comparison with other CA models, we can conclude that safety conditions are essential in modeling vehicular traffic and furthermore, this implies that drivers seem to take into account their vehicles braking limitations (at least unconsciously) while driving.

Finally, we thought of a second order model as one in which the safe distance of a car not only depends on its velocity, but also on the velocity of the leading car. This model would then take into account the braking limitations of the leading car too. This second order model leaves our analytical calculation for the backward speed of the downstream front of a traffic jam unchanged, however from the simulations carried out by now with this second order model, we have not found yet any remarkable different behavior, although this will still be considered for future work.

Acknowledgments

We would like to thank M. E. Larraga for the many enlightening discussions. This work was partially supported by UNAM, Grant No. PAPIIT IN102511. H.T. acknowledges the scholarship from CONACyT (Mexico). Computations have been performed at the Bakliz and Kanbalam computers of the Supercomputing Department of DGTIC-UNAM.

References

1. A. Schadschneider, D. Chowdhury and K. Nishinari, *Stochastic Transport in Complex Systems* (Elsevier, 2011).
2. D. Chowdhury, L. Santen and A. Schadschneider, *Phys. Rep.* **329**, 199 (2000).
3. J. Montemayor-Aldrete, P. Ugalde-Velez, M. del Castillo-Mussot, C. Vazquez-Villanueva, G. Vazquez and A. Mendoza-Allende, *Physica A* **361**, 630 (2006).
4. M. Larraga and L. Alvarez-Icaza, *Physica A* **389**, 5425 (2010).
5. K. Nagel and M. Schreckenberg, *J. Phys. I* (*France*) **2**, 2221 (1992).
6. D. Helbing, *Rev. Mod. Phys.* **73**, 1067 (2001).
7. T. Nagatani, *Rep. Prog. Phys.* **65**, 1331 (2002).
8. *Traffic Engineering Handbook* (Institute of Transportation Engineers, 1999).
9. S. Krauss, P. Wagner and C. Gawron, *Phys. Rev. E* **55**, 5597 (1997).
10. S. Krauss, Ph. D. Thesis, Deutsches Zentrum fuer Luft-und Raumfahrt (1998).

11. L. Neubert, L. Santen, A. Schadschneider and M. Schreckenberg, *Phy. Rev. E* **60**, 6480 (1999).
12. A. Schadschneider, *Physica A* **285**, 101 (2000).
13. M. E. Larraga, J. A. del Rio and A. Schadschneider, *J. Phys. A Math. Gen.* **37**, 3769 (2004).
14. V. Popkov and G. M. Schütz, *Europhys. Lett.* **48**, 257 (1999).